Future Integrative Medicine **2023** vol. 2(2) | 75–89
DOI: 10.14218/FIM.2023.00001

Original Article

Protective Effect of Dogwood Alcohol Extract on Hepatic Ischemia Reperfusion Injury based on Network Pharmacology and Transcriptomic Sequencing

Chengcheng Guo[1], Zirong Liu[2] and Hongsheng Liu[3*]

[1]*Department of Neurology, Tianjin First Central Hospital, Tianjin, China;* [2]*Hepatobiliary surgery, Tianjin First Central Hospital, Tianjin, China;* [3]*NHC Key Laboratory of Critical Care Medicine, Tianjin First Central Hospital, Tianjin, China*

Received: January 06, 2023 | **Revised:** February 20, 2023 | **Accepted:** June 08, 2023 | **Published online:** June 25, 2023

Abstract

Background and objective: Hepatic ischemia-reperfusion injury (HIRI) is a key factor leading to complications and poor prognosis after hepatobiliary surgery, but its pathogenesis remains unclear. Hence, it is a very necessary discovery the prevention and treatment methods and pathological mechanism of HIRI.

Methods: Our animal experiments indicated that two doses of dogwood alcohol extract (DAX) at 5 g/kg and 2.5 g/kg (crude drug/mouse body mass) could significantly reduce serum alamine aminotransferase (AST) and aspartate aminotransferase (ALT) in HIRI mice. The level of these two transaminases determined the pharmacodynamic effect of DAX on HIRI. Next, we used the results of network pharmacology and transcriptome sequencing to obtain important prevention and cure target genes, and applied molecular docking to simulate receptor and ligand binding. Finally, immunohistochemical method was made use of verifying the results.

Results: When the model group vs control group, administration group vs model group, set padj < 0.05, | log2FoldChange | >1.0 filter condition, the intersection between the obtained transcriptome sequencing data set and the network pharmacological target was only heparin-binding epidermal growth factor (HBEGF). Then DockThor online software was applied to make loganin and ursolic acid, small molecular compounds contained in DAX, form complexes with HBEGF active sites through hydrogen bonding to interfere with HIRI. Meanwhile, immunohistochemical test results showed that HBEGF expression decreased in the administration group compared with the model group (*$P < 0.05$).

Conclusions: DAX interferes with the occurrence and development of HIRI by down-regulating HBEGF. Our experimental results not only highlight the advantages of traditional Chinese medicine in treating difficult diseases, but also provide a reference for clinical exploration of new methods to prevent and treat HIRI.

Keywords: Dogwood Alcohol extract; Hepatic ischemia-reperfusion injury; HBEGF; network pharmacology; transcriptome sequencing.

Abbreviations: ALT, aspartate aminotransferase; AST, alamine aminotransferase; DAX, dogwood alcohol extract; EGF, epidermal growth factor; HBEGF, heparin-binding epidermal growth factor; HCC, hepatocellular carcinoma; HIRI, hepatic ischemia-reperfusion injury; PD, anti-Parkinson's disease; TCM, Traditional Chinese Medicine.

***Correspondence to**: Hongsheng Liu, NHC Key Laboratory of Critical Care Medicine, Tianjin First Central Hospital, Tianjin 300192, China. ORCID: https://orcid.org/0000-0002-4186-6826. Tel: +86 13388092828, E-mail: lhswmg@sina.com

How to cite this article: Guo C, Liu Z, Liu H. Protective Effect of Dogwood Alcohol Extract on Hepatic Ischemia Reperfusion Injury based on Network Pharmacology and Transcriptomic Sequencing. *Future Integr Med* 2023;2(2):75–89. doi: 10.14218/FIM.2023.00001.

Introduction

Hepatic ischemia-reperfusion injury (HIRI) is a two-phase process of ischemia-induced cell damage and reperfusion-induced inflammatory reaction,[1] which is an inevitable process during liver transplantation, liver resection and other operations, and an important cause of early graft failure, tissue damage, organ rejection and even transplant failure.[2,3] However, unfortunately, the mechanism of HIRI is still unclear, and there are no effective prevention and treatment methods in clinic.[4] Therefore, it is imperative to elucidate its mechanism of action and develop new drugs to treat HIRI targets.

At present, the mechanism of HIRI is mainly studied in these aspects, such as: cell energy metabolism disorder, ion distribu-

tion imbalance,[5] oxidative stress,[6] poor blood circulation,[7] cell apoptosis,[8] *etc.* For the time being, the main intervention methods for HIRI include reducing the time of hilar occlusion, hypothermia therapy, drug pretreatment, drug intervention, and the use of various inhibitors and antagonists.[9] Nonetheless, these research thoughts and approaches are not the best way to intervene in HIRI, and it is imperative to further probe the ways to prevent and treat HIRI.

Traditional Chinese Medicine (TCM) is a shining point in the world medical field. China should continue to tap its potential for the benefit of mankind. Recent studies have shown that some TCM monomers, as preprocessing drugs, can act a vital role in the progress of HIRI. For example, Gao *et al.* have certain anti-inflammatory and antioxidant effects on HIRI by regulating ROS and TLR-4-NF-kappa B pathways.[10] He *et al.* showed that resveratrol pretreatment protects hepatocytes from HIRI through toll-like receptor 4/ nuclear factor-Kappa B signaling pathway in vitro and in vivo.[11] Zhang *et al.* salidroside achieved its defending effect on HIRI by inhibiting the apoptosis of hepatocytes.[12] However, HIRI is a complicated pathological course, and its nosogenesis is multi-directional . As a consequence, studies on the mechanism of single ingredient corresponding to single target gene cannot perfect settle the adverse factors of HIRI in hepatic surgery, indicating the limitation of the drug's effects. Therefore, the characteristics of multi-components, multi-targets and multi-effects of TCM just intervene in the multi-directional, multi-level and multi-mechanism complicated pathological process caused by HIRI. In 2007, British pharmacologist Hopkins proposed the concept of "network pharmacology",[13] which expounded that the happen of diseases is the consequence of the break of the dynamic balance of multi-gene, multifunctional protein and multi-pathway interactions in human body.[14] That is to say, based on the method of bioinformatics, network pharmacology can predict and reveal the interrelationship between the active ingredients of drugs and the targets of related diseases more deeply and systematically through the cross-application of multiple disciplines, and explain the molecular mechanism of TCM disease prevention and treatment, so as to provide help for the clinical treatment of difficult diseases.[15]

Dogwood is an important Chinese medicinal material with sour and astringent taste. It has a wide range of pharmacological activities, such as protecting liver and kidney, protecting heart, anti-oxidation, anti-inflammation, anti-aging, anti-forgetting, anti-osteoporosis, anti-depression and immune regulation, and is a common ingredient in many TCM prescriptions.[16] According to modern pharmacological studies, about 90 compounds have been isolated and identified from dogwood, and secondary metabolites such as terpenoids, flavonoids, tannins and polysaccharides exist in its fruits.[17] In this study, target genes corresponding to the three most important components loganin, ursolic acid and oleanolic acid were selected to explore the prevention and treatment mechanism of HIRI. XU *et al.* reported that it can alleviate the effect of angiotensin II-induced myocardial hypertrophy.[18] In addition, the study also found no significant adverse effects of loganin on normal cells and organs. In the study of nerve cell injury, loganin inhibited the production of reactive oxygen species in PC12 cells, inhibited the activity of Aβ-induced Caspase-3, and reduced cell apoptosis. Meanwhile, the activity of intracellular nuclear factor κB (NF-κB) signaling pathway and the phosphorylation level of mitogen-activated protein kinase (MAPK) are decreased to delay the process of development of Alzheimer's disease.[19] Some scholars have reported that loganin mainly reduces the level of MPTP-induced autophagosomes by increasing the digestive effect of lysosomes on autophagosomes in PC12 cells, thus playing a role in anti-Parkinson's disease (PD).[20] In addition, loganin has a good pharmacological effect in the prevention and treatment of diabetes,[21] synovial inflammation in rats,[22] intervention in the oxidative damage of ARPE-19 human retinal pigment epithelial cells,[23] and relief of gout inflammation.[24] Ursolic acid and oleanolic acid are isomers and therefore have similar physiological effects in terms of pharmacological activity. oleanolic acid and ursolic acid are widely present in many TCM plants, and contemporary pharmacological researches have revealed that they have intervention effects on neurodegenerative diseases, neuropsychiatric diseases and other brain diseases.[25] In addition, it also has good pharmacological activity in anti-ulcer, anti-hypertension, anti-obesity, anti-cancer and other aspects.[26] The ionic derivatives of oleanolic acid and ursolic acid have enhanced hydrophilicity, which can inhibit the growth activity of human hepatocellular carcinoma cell line (HepG2).[27] Oleanolic acid and ursolic acid have a good inhibitory effect on human lung cancer cell vitality.[28] Ursolic acid and oleanolic acid derivatives can well inhibit the activity of acetylcholinesterase and buylcholinesterase to ameliorate Alzheimer's disease.[29] Ursolic acid and oleanolic acid have been shown to have certain anti-cancer effects on various types of tumors, especially on tumors formed in the gastrointestinal tract, such as gastric cancer, colorectal cancer, pancreatic cancer and liver cancer.[30] In view of the extensive pharmacological activities of dogwood reported above, it will be of great relevance to continue to discuss its efficacy in other difficult diseases.

Our animal experiments clarified that HIRI + DAX group could significantly reduce the expressions of AST and ALT in serum of mice, and there were significant differences compared with HIRI group ($^{**}P < 0.01$), indicating that DAX could effectively protect HIRI in mice. Therefore, we continue to use network pharmacology and transcriptomic sequencing to explore the potential mechanism of DAX to alleviate HIRI occurrence, to provide theoretical reference for clinical development of new drugs to protect HIRI.

Materials and methods

Animal and drug therapy

The animals used in the experiment were provided by the Institute of Experimental Animals of the Chinese Academy of Medical Sciences (license number: SCXK (Jing) 2014-0004). The study was reviewed and approved by Animal Ethics Committee of Nankai University. The animals were male C57BL mice aged 5–6 weeks and weighing 19–22 g, kept in an air-conditioned SPF environment. The temperature was controlled at 23 ± 1.0°C and the humidity was controlled at 50 ± 10°C, and the mice could eat and drink freely.

DAX preparations (containing loganin 2.498 mg/mL, ursolic acid 0.1316 mg/mL, oleanolic acid 0.160 mg/mL) were provided by Key Laboratory of Critical Care and Emergency Medicine of the National Health Commission (Tianjin, China). High and low doses of 5 g/kg and 2.5 g/kg (crude drug/mouse body weight) were administered intragastrically.

35 mice were randomly divided into 5 groups with 7 mice in each group, which were Sham operation group (Sham), Sham + HDAX high-dose group (Sham + HDAX), model group (HIRI), model group + DAX low-dose group (HIRI + LDAX), and model group +DAX high-dose group (HIRI + HDAX). Sham+ HDAX, HIRI+ LDAX and HIRI+ HDAX were given DAX intragastric administration (ig) once a day for 7 days, and the other Sham and HIRI model groups were given the same amount of normal saline intragastric administration. 1 h after the final administration of pretreatment, mice were anesthetized with pentobarbital sodium (40

ng/g) by ip (IP), the abdominal cavity was opened in the middle of the upper abdomen, the liver was carefully exposed, and the porta hepatis was dissociated. HIRI, HIRI + LDAX and HIRI + HDAX groups clamped the left lobe and middle lobe of liver into the hepatic vessels to block blood flow, and released the vascular clips 1 h later to restore blood flow (Sham and Sham + HDAX groups only free the hepatic portal and did not block blood flow). 6 h after reperfusion, blood was collected from the eyeball. Part of the liver tissue was isolated and stored at −80 °C, while the other part was stored at 10% formalin.

Serum biochemical analysis and histopathological examination of the liver

First, the collected mouse blood was left to stand at room temperature for 60 min and centrifuged at 3 000 r/min for 20 min to separate the serum. Then, the levels of AST and ALT in serum of mice were measured by Sysmex CHEMIX-180 developed by Tianjin First Central Hospital, P. R. China.

The liver tissues of each experimental group were taken from 10% formalin for histopathological examination. The sample was first fixed in a 4% paraformaldehyde buffer solution and then embedded in paraffin wax. Then the sample was sliced 5μm, dewaxed with xylene and ethanol, hematoxylin and eosin (HE) staining, and dehydrated. Finally, the sections were observed with a microscope, and the histological changes were observed at a randomly selected 200-times microscope.

Construction of active ingredient-HIRI target gene network

It is known from the literature that loganin, ursolic acid and oleanolic acid are the main active components of DAX that play a good pharmacological effect.[31–34] Therefore, we studied these three components in DAX. First of all, in TCM database and analysis platform system pharmacology TCMSP (http://tcmspw.com./tcmsp.php) to obtain the DAX loganin, ursolic acid and oleanolic acid related small molecular compound structure. Then, using the Pharm Mapper (http://lialb-ecust.cn/pharmmapper/), Swiss Target Prediction (http://www.swisstarget predication.ch /) database predicts their corresponding target genes. The obtained target genes were merged, and the duplications were removed and unified on the UniProt service platform (http://www.uniprot.org/) for total sum transformation. Finally, the target database of three DAX active ingredients was established and represented by UniProt ID. Then in GeneCards (http://www.genecards.org/) on the database with "hepatic ischemia reperfusion injury" as keywords to predict the target genes associated with HIRI, and in the transformation in the UniProt service platform, Finally, it is represented by the UniProt ID. Collecting the intersection target genes of DAX components and HIRI application Cytoscape3.7.2 Software Mapping Active Components-Visual network diagram of HIRI disease target genes.

KEGG path analysis

The intersection target gene of component-HIRI was set as Homo sapiens in the form of Uniprot. KEGG (Kyoto Encyclopedia of Genes and Genomes) enrichment analysis was conducted using metascape (http://metascape.yuuorg/) online database. KEGG enrichment data sets were obtained with $^{**}P < 0.01$ as the screening condition.

RNA-seq experiment

Three samples (n = 3) were selected from each of the above three experimental groups (Sham, HIRI, HIRI +LDAX) through RNA-seq experiment. First, RNA was extracted from liver tissues and purity, concentration and integrity of the RNA samples were tested for quality control. Second, oligo dT2 magnetic beads were used to bind specifically to the poly (A) tail of mRNA to remove other RNA, and the purified mRNA was fragmented using fragmentation reagent. Finally, the first strand of cDNA was synthesized in M-MuLV reverse transcriptase system using fragmented mRNA as template and random oligonucleotide as primer. Then RNaseH was used to degrade the RNA strand, and the second cDNA strand was synthesized from dNTPs in the DNA polymerase I system. The purified double-strand cDNA was end-repaired, A tail was added and sequencing joints were connected. cDNA about 250–300 bp was screened by AMPure XP beads, and PCR amplification was performed and the PCR products were purified again using AMPure XP beads to obtain the library. Then, Illumina sequencing was performed after qualified library check.

DAX interferes with the acquisition of HIRI hub target genes

We set the data of the RNA-seq experiment to padj < 0.05, | log2FoldChange | > 1.0 filter condition, obtain the effective raised or lowered target genes and network pharmacology components-HIRI target genes in intersection, the intersection of the target genes is the DAX protect HIRI hub target genes.

Molecular docking simulation verification

The three-dimensional structure of the hub protein obtained in "2.5" above was obtained through the PDB (http://www.rcsb.org/) database. The SPF structure of small molecule compounds corresponding to hub proteins was obtained from PubChem database (https://pubchem.ncbi.nlm.nih.gov/). At the same time, the application of DockThor (https://dockthor.lncc.br/v2/) online tools for molecular docking. Verify the binding state of the protein receptor to the small molecule compound ligand.

Heparin-binding epidermal growth factor (HBEGF) were verified by immunohistochemistry

First, mouse liver tissue was sliced and dewaxed into water and then placed in a microwave oven for antigen repair. Second, the slices were incubated in 3% hydrogen peroxide solution at room temperature and away from light for 25 minutes. Thirdly, 3% BSA was added and closed at room temperature for 30 min. Then, the blocking liquid was gently shaken off and HBEGF (1:200, ABclonal Wuhan, China) antibody diluted with PBS was added, and incubated overnight at 4°C. Fourth, the sections were covered with the secondary antibody corresponding to the primary antibody labeled by HRP and incubated at room temperature for 50 min. Fifth, the sections were washed with PBS and then freshly prepared DAB color developing solution was added. Finally, the nucleus was reversely stained with hematoxylin, dehydrated and sealed.

Data analysis

Statistical analysis was performed by GraphPad 8.0.2 software. The experimental values of each group were analyzed by one-way ANOVA and Tukey's post-hoc statistics, and expressed as mean ± standard error ($\bar{x} \pm s$) (n = 3). $^{*}P < 0.05$ was considered statistically significant.

Result

Biochemical and HE test results

The biochemical detection results showed that compared with the

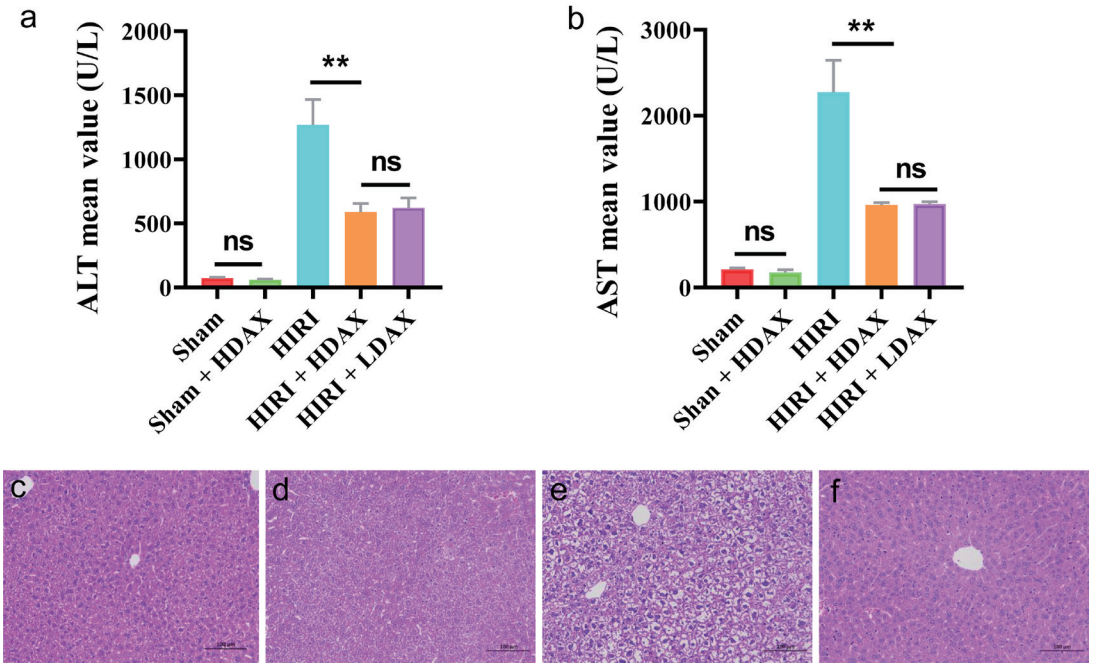

Fig. 1. Biochemical and HE test results. (a–b) indicates the effect of DAX on HIRI by biochemical detection of AST and ALT; (c–f) the result of HE detection. (c) Sham; (d) Sham + HDAX, (e) HIRI; (f) HIRI + LDAX. DAX, dogwood alcohol extract; HIRI, hepatic ischemia-reperfusion injury.

Sham group, the serum ALT and AST levels in the HIRI model group were significantly increased ($^{**}P < 0.01$), indicating successful modeling. Compared with HIRI model group, serum ALT and AST levels in HIRI + LDAX and HIRI + HDAX groups were significantly decreased ($^{**}P < 0.01$), indicating that DAX had a protective effect on HIRI mice, and proving the pharmacodynamic effect of DAX. Sham was compared with Sham + HDAX group, the changes of ALT and AST were not statistically significant ($P > 0.05$), indicating that DAX did not cause damage to normal mouse liver tissue, indicating the safety of DAX. There was no statistical significance between high and low doses of DAX, namely HIRI +LDAX and HIRI +HDAX ($P > 0.05$). The results showed that A dose range of 2.5 to 5 g/kg (drug/mouse body weight) could protect HIRI in mice, but there was no dose dependence, as shown in Fig. 1 (a–b).

HE staining showed that compared with Sham group, liver tissues of mice in HIRI group showed different degrees of steatosis, inflammatory cell infiltration and swelling/necrosis. Compared with HIRI group, liver cells in HIRI + LDAX group were round and full, and no obvious inflammatory changes were observed. Thus, the pathological phenomenon of liver tissue was reversed and improved, indicating that DAX had an intervention effect on HIRI in mice. The liver tissue of mice in Sham and Sham + HDAX group had little change, indicating that DAX basically did not cause damage to normal mouse liver tissue, as shown in Figure 1c–f.

Results of network pharmacological analysis

Active ingredient -HIRI network mapping results: The three small molecule compound structures of loganin, ursolic acid and oleanolic acid contained in DAX downloaded from TCMSP were uploaded to the Pharm Mapper service platform in MOL2 format for target prediction. Meanwhile, the SMILES of chemical constituents of loganin, ursolic acid and oleanolic acid were uploaded to the Swiss Target Prediction database platform for target prediction. Then, the targets were collected and represented by UniProt ID after sorting and removing duplicates. Finally, a total of 613 predicted targets of DAX were obtained.

A total of 1117 target genes were obtained in the GeneCards database using the keyword “hepatic ischemia injury”, and is expressed as UniProt ID. 613 components and the predicted target genes in intersection, get 87 intersection target genes, and then use Venny2.1 (http://bioinfogp.cnb.csic.es/tools/venny/index.html) software will its visualization, as shown in Figure 2a. Cytoscape 3.7.2 software was applied to make the composition-HIRI network mapping view. Pink nodes represent DAX small molecular compounds, green nodes represent HIRI-related target genes, and blue lines represent the intersection lines between components and disease target genes, as shown in Figure 2b.

Pathway analysis: The top 20 KEGG pathways were obtained for 87 intersection target genes using metascape online database with $^{**}P < 0.01$ as the screening condition, as shown in Figure 2c. As shown in the figure, the PI3K-Akt signaling pathway is one of the most important pathways. The PI3K-Akt signaling pathway with the best score contains 10 target genes. EPHA2 (P29317), MTOR (P42345), HSP90AA1 (P07900), IL6 (P05231), IL2 (P60568), MDM2 (Q00987), NGFR (P08138) MAPK3 (P27361), RAC1 (P63000), VWF (P04275), as shown in Figure 3.

Prevention of hub target gene acquisition in HIRI by DAX

Results of RNA-seq analysis: According to the experimental results of RNA-seq, HIRI vs Sham, (HIRI + LDAX) vs HIRI between groups, set padj < 0.05, | log2FoldChange | >1.0 filter condition, 50 down-regulated target genes of DAX intervention in HIRI were obtained. In addition, padj is a correction for the hypothesis test P-value to control the proportion of false positives, as shown in Figure 4a and Table 1.

87 intersection target Gene maps of Component-HIRI: The 87

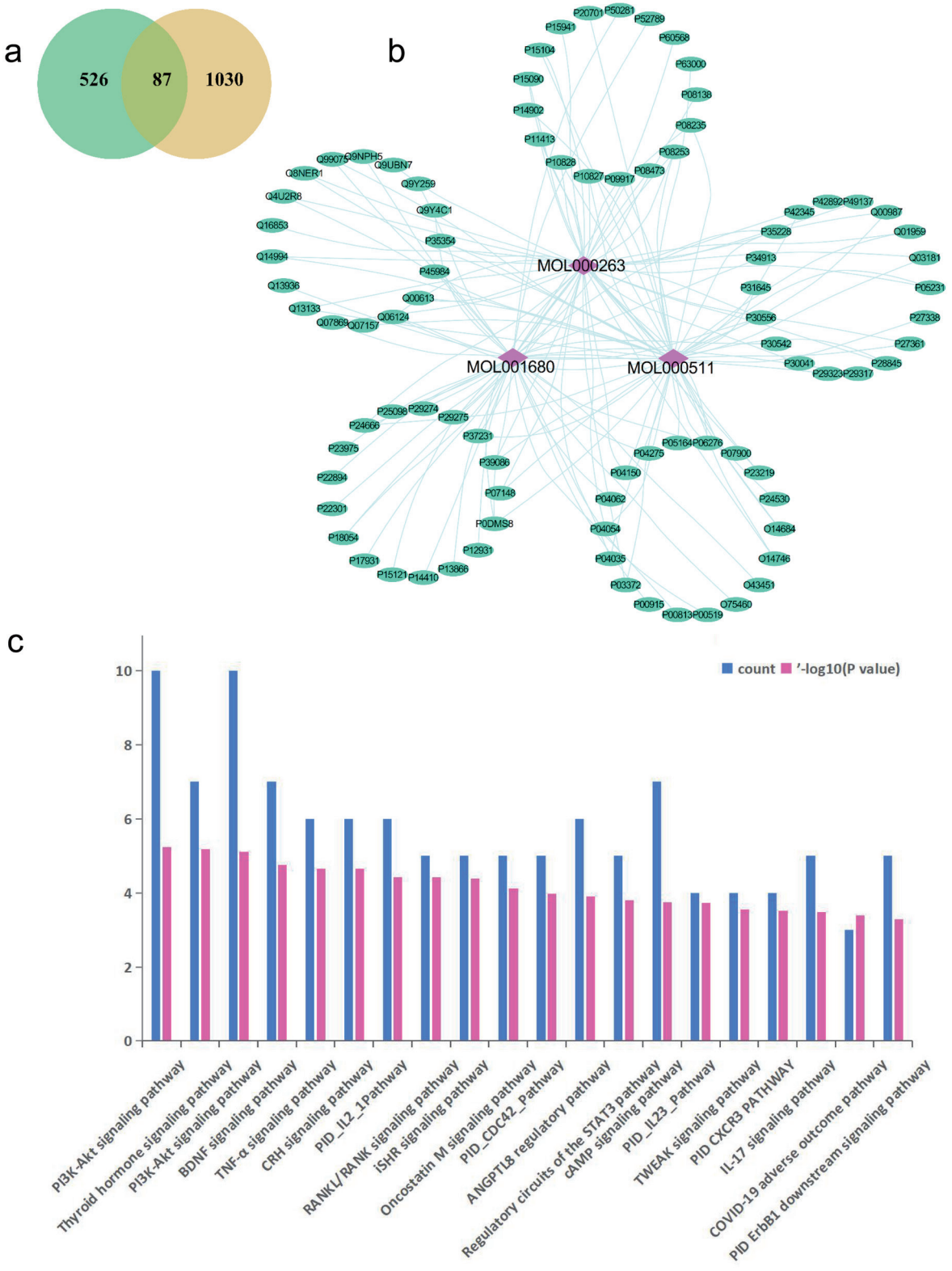

Fig. 2. Results of network pharmacological analysis. (a) the intersection diagram of component and HIRI target. Green indicates the number of constituent targets and yellow indicates the number of HIRI targets; (b) the mapping map between components and HIRI network; (c) Schematic diagram of KEGG pathway of 87 intersection target genes. ANGPTL8, Angiopoietin-like protein 8; BDNF, Brain-derived neurotrophic factor; CRH, Corticotropin-releasing hormone; HIRI, hepatic ischemia-reperfusion injury; iSHR, intracellular steroid hormone receptor; TWEAK, TNF-related weak inducer of apoptosis.

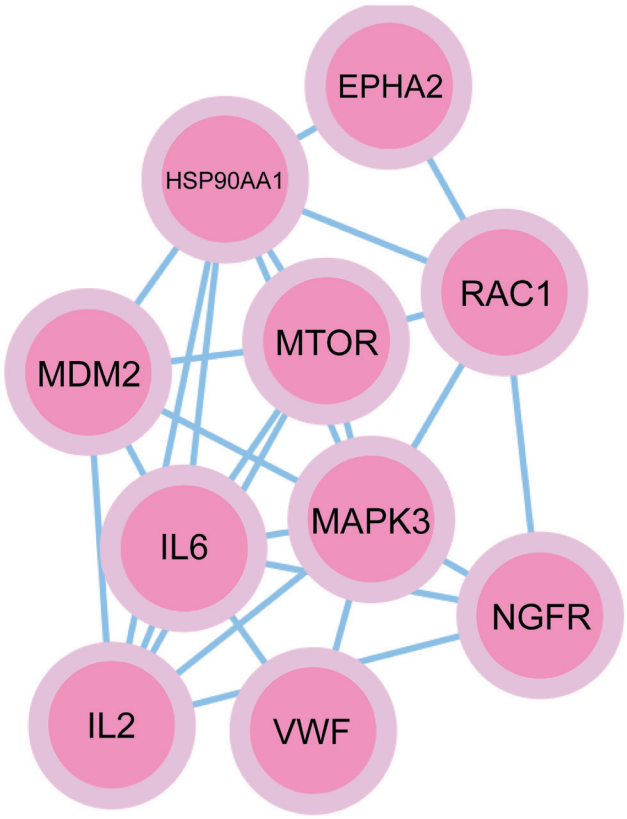

Fig. 3. The PI3K-Akt pathway constructed via Cytoscape contains 10 target genes.

intersection target genes of component-HIRI obtained through database were imported into STRING (https://string-db.org/) online database to obtain the corresponding data set. This data set is then imported into Cytoscape software to visualize it, as shown in Figure 4b.

The intersection of target genes contained in Figure 4a and b was taken to obtain HBEGF, as shown in Figure 4c. That is, HBEGF is the hub target gene that DAX protects HIRI.

The binding status of ligand and receptor was verified by molecular docking

The crystal structure of HBEGF protein was obtained using PDB database and uploaded to DockThor online molecular docking tool. At the same time, 3D structures of loganin, ursolic acid and oleanolic acid have been downloaded from PubChem database and uploaded to DockThor in sdf form. Click Blind Docking to establish an active site, and molecular docking can be carried out with corresponding HBEGF protein crystal structure. The results showed that loganin combined with the active site of HBEGF (PDB ID 2m8s) through four hydrogen bonds to form a complex, and ursolic acid combined with the active site of HBEGF through three hydrogen bonds to form a complex, as shown in Figure 4d-e.

HBEGF experiment verified the results

The sections of Sham, HIRI and (HIRI + LDAX) groups (n = 3) were immunostained with HBEGF (1:200) antibody. Histochemistry score (H-score) was used to convert the positive number and staining intensity of each section into corresponding values, so as to achieve the purpose of semi-quantitative tissue staining. The results showed that the expression of HBEGF in HIRI group was significantly increased compared with that in Sham group (***P* < *0.01*), indicating that the target genes were low expressed in normal liver tissues and high expressed in HIRI. Compared with HIRI group, the expression of HBEGF in (HIRI + LDAX) group was decreased (**P* < *0.05*), indicating that DAX could protect HIRI by reducing the expression of the target genes (Fig. 5b).

Discussion

The function of liver tissues and organs can be restored after most liver ischemia-reperfusion. However, sometimes after liver ischemia-reperfusion, liver tissues and organs can not only recover, but also aggravate the structural disorders and functional injuries of liver tissues. Therefore, it is of great significance to actively explore how to reduce cell dysfunction and tissue damage caused by HIRI. Dogwood is a rare traditional Chinese medicinal material. It belongs to the two classics of liver and kidney. It can not only benefit the essence, but also help the Yang. The main active components of Dogwood are ursolic acid, oleanolic acid and loganin. Therefore, in this study, the corresponding targets of these three components were used to explore the mechanism of HIRI.

Our animal experiments showed that DAX can significantly reduce the expression of AST and ALT in serum of HIRI mice, indicating that DAX can interfere with HIRI. Then, we applied network pharmacology and RNA-seq experimental data mining to find that HBEGF is a therapeutic target for prevention and treatment of HIRI. That is, DAX protects the occurrence and development of HIRI by down-regulating the expression of HBEGF.

HBEGF is first synthesized as a transmembrane precursor (pro-HBEGF), and then it converts to the soluble protein (s-HBEGF) of 14–20 kDa via enzyme cutting and being released. Pro-HBEGF is affected by all kinds of proteins, and it can be shed into active s-HBEGF. S-HBEGF plays a major role in physiological and pathological conditions of the body.[35,36] In our study, HBEGF promoted the growth of ischemia-induced hepatocyte injury and perfusion-induced inflammatory cells by enhancing its binding strength with mouse liver target cells. After the intervention of HIRI mice with DAX, the small molecular compounds loganin and ursolic acid contained in DAX form complexes by binding with the active sites of HBEGF target genes, thus reducing the expression of HBEGF in liver tissues, eliminating and restoring part of inflammatory cells and damaged liver cells. To achieve the effect of protecting HIRI. Meanwhile, it provides a new intervention target for clinical treatment of HIRI.

In addition, we found associated target genes interacting with HBEGF using the STRING database (https://string-db.org/). Among them, the combined score of HBEGF, EGFR, ERBB4 and ERBB2 is greater than 0.99, indicating a close correlation between them, that is, they have similar physiological functions in the body. Besides, the combined scores of HBEGF, CD9, CD44 and MMP9 were all greater than 0.98, indicating that they play similar roles in the body (Fig. 6). These target genes which are closely related to HBEGF will be the focus of our further research.

Current studies have shown that epidermal growth factor (EGF) is involved in the development process of various diseases, such as lung cancer,[37] colon cancer and rectal cancer,[38] *etc.* Heparin-binding epidermal growth factor (HBEGF), a member of EGF family, has similar structure and biological function to EGF. HBEGF is the upstream ligand of EGFR pathway. Some studies have shown that HBEGF plays an important regulatory role in the process of

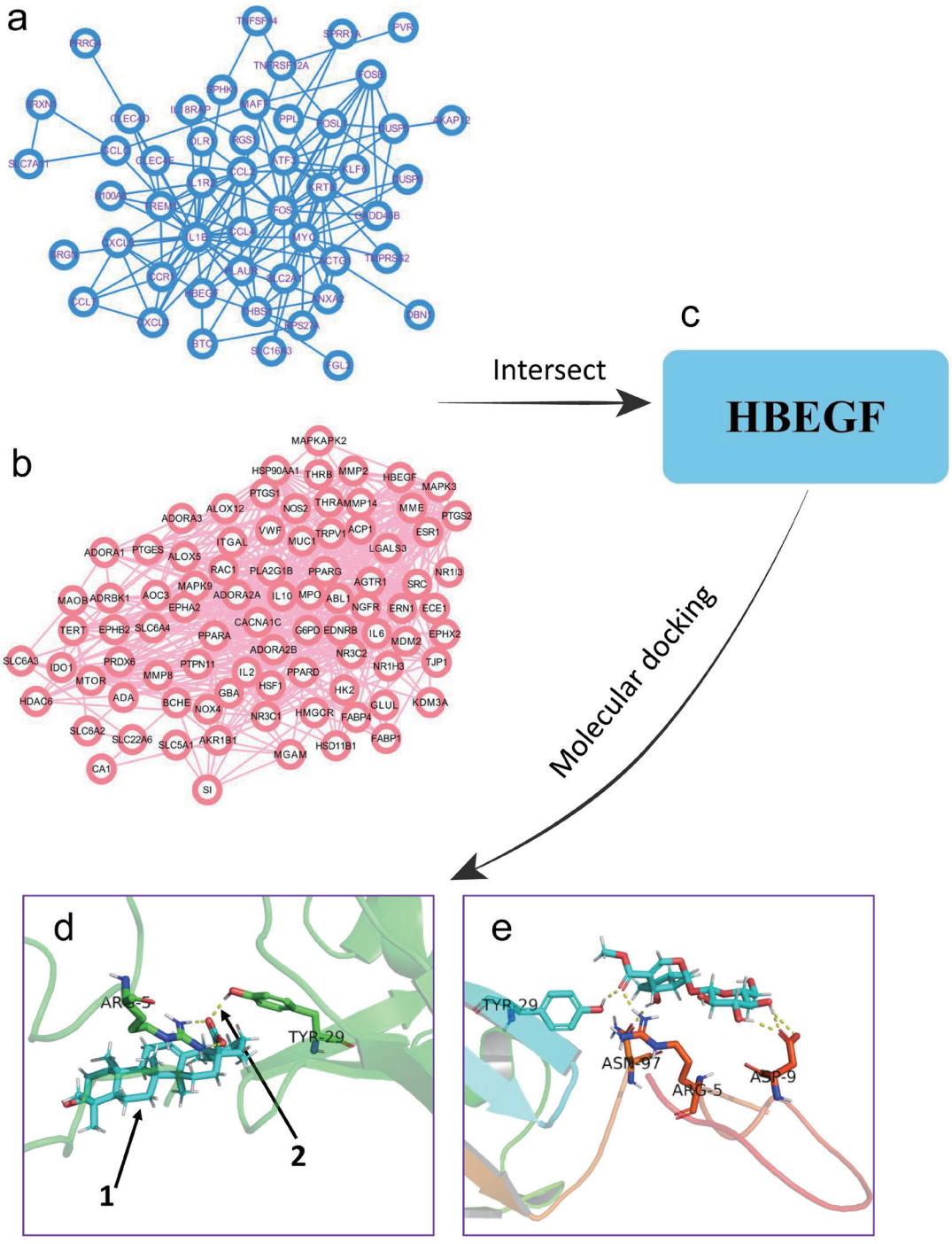

Fig. 4. Result diagram. (a) Results of RNA-seq analysis; (b) 87 intersection target Gene maps of Component-HIRI; (c) HBEGF is the hub target gene that DAX protects HIRI; (d) 1 is the ligand, 2 is the receptor protein. As shown in the figure, loganin binds to the active site of HBEGF through four hydrogen bonds to form a complex; (e) ursolic acid binds to the active site of HBEGF through three hydrogen bonds to form a complex. DAX, dogwood alcohol extract; HBEGF, heparin-binding epidermal growth factor; HIRI, hepatic ischemia-reperfusion injury.

tumor proliferation, apoptosis and invasion by activating the corresponding receptor EGFR and multiple downstream signaling pathways.[39] HBEGF is a glycosylated protein named for its high heparin affinity. Li *et al.* reported that HBEGF may induce the proliferation and migration of lung fibroblasts by inducing airway epithelial cells IL-8,[40] thus participating in the pathological process of airway fibrosis. Salama *et al.* reported that after studying the effects of aloe essential oil on melanoma growth and tumor cell migration,[41] it was found from the mechanism that aloe essential oil could be used as a single therapy or combined with marrow

Table 1. RNA-seq result

Grouping	Log2FoldChange	Padj	Gene_name	Up or down
HvsS	−1.377782765	0.037823571	Col15a1	down
HDvsH	1.461402704	0.003548056	Col15a1	up
HvsS	−1.076701705	0.001754356	Gm7336	down
HDvsH	1.023177196	0.009128492	Gm7336	up
HvsS	1.476377015	0.000188218	Actg1	up
HDvsH	−1.146461975	0.008129323	Actg1	down
HvsS	4.49209096	3.38E-10	Adam8	up
HDvsH	−1.803797918	0.002001431	Adam8	down
HvsS	2.984783063	1.17E-10	Akap12	up
HDvsH	−2.238313629	7.12E-06	Akap12	down
HvsS	1.189715336	0.029935413	Anxa2	up
HDvsH	−1.318887138	0.04553979	Anxa2	down
HvsS	2.334848967	0.001181242	Arntl2	up
HDvsH	−1.82757496	0.016458714	Arntl2	down
HvsS	5.692773408	1.79E-17	Atf3	up
HDvsH	−2.809872624	0.007664624	Atf3	down
HvsS	1.834386105	0.008552665	Btc	up
HDvsH	−1.911147269	0.013679165	Btc	down
HvsS	3.070294982	8.94E-09	Ccl2	up
HDvsH	−1.835051048	0.006460953	Ccl2	down
HvsS	4.28129749	3.45E-05	Ccl4	up
HDvsH	−2.41438031	0.017468321	Ccl4	down
HvsS	4.717077235	1.88E-06	Ccl7	up
HDvsH	−1.928531243	0.021421183	Ccl7	down
HvsS	5.35087837	2.05E-15	Ccr1	up
HDvsH	−1.497468862	0.016106379	Ccr1	down
HvsS	2.056556547	0.000182136	Cda	up
HDvsH	−1.337493082	0.030210068	Cda	down
HvsS	3.93324288	3.44E-07	Ch25h	up
HDvsH	−1.483907107	0.041429946	Ch25h	down
HvsS	6.38829675	2.61E-13	Clec4d	up
HDvsH	−1.540615196	0.013127103	Clec4d	down
HvsS	5.602987704	6.49E-13	Clec4e	up
HDvsH	−1.58758556	0.020122055	Clec4e	down
HvsS	3.710266744	4.86E-16	Ctla2a	up
HDvsH	−1.14972139	0.02187684	Ctla2a	down
HvsS	7.605137853	2.13E-06	Cxcl3	up
HDvsH	−3.936082933	0.001359328	Cxcl3	down
HvsS	4.17454269	0.003365218	Cxcl5	up
HDvsH	−2.75916468	0.047495317	Cxcl5	down
HvsS	2.649452722	4.02E-12	Dbn1	up

(continued)

Table 1. *(continued)*

Grouping	Log2FoldChange	Padj	Gene_name	Up or down
HDvsH	−1.106148499	0.017499056	Dbn1	down
HvsS	2.575676885	7.31E-06	Dusp5	up
HDvsH	−2.270904035	0.000512963	Dusp5	down
HvsS	1.474143835	0.007871251	Dusp6	up
HDvsH	−1.71704274	0.002769285	Dusp6	down
HvsS	1.037380933	0.036019245	Fam214b	up
HDvsH	−1.043174239	0.005437207	Fam214b	down
HvsS	1.190254108	0.005426971	Fgl2	up
HDvsH	−1.140010286	0.005811932	Fgl2	down
HvsS	3.072836814	0.014948658	Fos	up
HDvsH	−2.325693246	8.55E-05	Fos	down
HvsS	5.102965343	2.98E-05	Fosb	up
HDvsH	−4.469443299	0.034901265	Fosb	down
HvsS	4.655628905	3.73E-08	Fosl1	up
HDvsH	−3.497506842	8.76E-05	Fosl1	down
HvsS	1.803665808	0.010103383	Fst	up
HDvsH	−2.134170768	0.003599724	Fst	down
HvsS	3.880644116	0.004033456	Gadd45b	up
HDvsH	−2.995349539	0.009740321	Gadd45b	down
HvsS	1.214496871	0.008577924	Gclc	up
HDvsH	−1.369777957	0.00550169	Gclc	down
HvsS	2.139503237	2.20E-06	Gja4	up
HDvsH	−1.296119848	0.007983142	Gja4	down
HvsS	1.861319851	0.000625362	Glipr2	up
HDvsH	−1.634489709	0.010677727	Glipr2	down
HvsS	1.670973942	0.003970283	Gm10925	up
HDvsH	−1.302829406	0.042495007	Gm10925	down
HvsS	1.281233001	0.047660913	Gm28437	up
HDvsH	−1.324916529	0.038673535	Gm28437	down
HvsS	1.52271929	0.003870472	Haus8	up
HDvsH	−2.077896667	0.000512963	Haus8	down
HvsS	1.978855041	0.000830835	Hbegf	up
HDvsH	−1.948087561	0.011774753	Hbegf	down
HvsS	5.232134296	2.87E-05	Hilpda	up
HDvsH	−3.318208676	0.018696136	Hilpda	down
HvsS	1.035947503	0.010264434	Hmga1	up
HDvsH	−1.654453774	2.71E-05	Hmga1	down
HvsS	2.879483747	1.38E-08	Il18rap	up
HDvsH	−1.303135513	0.030210068	Il18rap	down
HvsS	3.396663097	1.22E-16	Il1b	up
HDvsH	−1.311685106	0.021016883	Il1b	down

(continued)

Table 1. *(continued)*

Grouping	Log2FoldChange	Padj	Gene_name	Up or down
HvsS	7.784590354	3.60E-14	Il1r2	up
HDvsH	−1.923344257	0.000703337	Il1r2	down
HvsS	3.547599429	4.95E-06	Kcne4	up
HDvsH	−2.343659526	0.003204425	Kcne4	down
HvsS	3.217449747	8.07E-13	Klf6	up
HDvsH	−1.740646871	0.000945294	Klf6	down
HvsS	2.209417234	1.86E-06	Krt8	up
HDvsH	−1.46239626	0.017499056	Krt8	down
HvsS	3.34251976	1.57E-25	Lilr4b	up
HDvsH	−1.400477374	0.000376344	Lilr4b	down
HvsS	2.728054166	5.87E-07	Maff	up
HDvsH	−1.912619981	0.001326666	Maff	down
HvsS	1.350809913	0.029757687	mt-Nd3	up
HDvsH	−1.235333983	0.026395214	mt-Nd3	down
HvsS	6.548114588	7.27E-08	Mup-ps21	up
HDvsH	−6.434085359	0.000703337	Mup-ps21	down
HvsS	2.995061615	1.33E-07	Myc	up
HDvsH	−1.863572597	0.003750843	Myc	down
HvsS	5.358877337	0.000187157	Olr1	up
HDvsH	−2.462977495	0.024307546	Olr1	down
HvsS	1.095820731	0.046079922	Pde4b	up
HDvsH	−1.372224957	0.047077594	Pde4b	down
HvsS	3.808494099	1.42E-09	Plaur	up
HDvsH	−1.241141126	0.04553979	Plaur	down
HvsS	1.669762912	0.000837702	Ppl	up
HDvsH	−1.344256091	0.032655691	Ppl	down
HvsS	3.783229293	3.95E-08	Prrg4	up
HDvsH	−1.696131176	0.034941274	Prrg4	down
HvsS	3.346880594	2.63E-15	Ptp4a1	up
HvsS	3.851769241	1.61E-14	Ptp4a1	up
HDvsH	−1.432444773	0.013127103	Ptp4a1	down
HvsS	2.574557027	1.94E-06	Pvr	up
HDvsH	−1.647413882	0.00550169	Pvr	down
HvsS	4.43906427	6.91E-07	Ramp3	up
HDvsH	−2.105566989	0.042908429	Ramp3	down
HvsS	1.603206454	2.20E-06	Rasip1	up
HDvsH	−1.013923694	0.013939765	Rasip1	down
HvsS	2.25474854	6.77E-05	Rell1	up
HDvsH	−1.668696849	0.017468321	Rell1	down
HvsS	3.609600116	9.56E-12	Rgs1	up
HDvsH	−1.460576738	0.0148487	Rgs1	down

(continued)

Table 1. *(continued)*

Grouping	Log2FoldChange	Padj	Gene_name	Up or down
HvsS	1.91596588	2.28E-05	Rps27a	up
HDvsH	−1.732526404	0.000780707	Rps27a	down
HvsS	5.319941887	1.43E-19	S100a8	up
HDvsH	−1.511923451	0.045087952	S100a8	down
HvsS	1.178698222	0.025959721	Samd4	up
HDvsH	−1.726046973	0.000558714	Samd4	down
HvsS	2.741425443	1.67E-05	Slc16a3	up
HDvsH	−1.590965504	0.036019191	Slc16a3	down
HvsS	1.19069827	0.019801308	Slc2a1	up
HDvsH	−1.218770091	0.003204425	Slc2a1	down
HvsS	5.471999827	2.70E-08	Slc7a11	up
HDvsH	−1.935910265	0.034941274	Slc7a11	down
HvsS	2.023639664	0.00785987	Smim3	up
HDvsH	−1.978368125	0.011934568	Smim3	down
HvsS	3.492304421	2.10E-08	Sphk1	up
HDvsH	−2.085614988	0.000106721	Sphk1	down
HvsS	3.840240659	2.12E-05	Sprr1a	up
HDvsH	−3.043728218	0.029216834	Sprr1a	down
HvsS	2.657167014	1.65E-10	Srgn	up
HDvsH	−1.646048585	0.000512963	Srgn	down
HvsS	2.487765034	8.54E-10	Srxn1	up
HDvsH	−1.986500177	1.19E-05	Srxn1	down
HvsS	5.434212809	1.46E-08	Stc1	up
HDvsH	−2.435283146	0.000257416	Stc1	down
HvsS	5.08089515	1.06E-27	Thbs1	up
HDvsH	−2.049299996	0.001850178	Thbs1	down
HvsS	2.629984328	8.89E-08	Tmprss2	up
HDvsH	−1.402124067	0.001990898	Tmprss2	down
HvsS	3.225317847	1.19E-07	Tnfrsf12a	up
HDvsH	−1.789790227	0.002142748	Tnfrsf12a	down
HvsS	4.49585254	1.22E-08	Tnfsf14	up
HDvsH	−1.747672392	0.031384022	Tnfsf14	down
HvsS	2.01487306	4.88E-05	Tox	up
HDvsH	−1.660649477	0.034304059	Tox	down
HvsS	6.951826095	4.98E-08	Trem1	up
HDvsH	−1.52335009	0.034379038	Trem1	down

suppressor drugs to treat melanoma, by blocking the HBEGF-induced EGFR signaling pathway and inhibiting the phosphorylation of ERK1/2. Gu *et al.* reported that age-related macular degeneration, mainly wet macular degeneration, is the main cause of irreversible vision loss worldwide.[42] Choroidal neovascularization is the characteristic pathological manifestation of wet age-related macular degeneration. In this study, gardeniin reduced transcription and expression of HBEGF in hypoxic-exposed retinal pigment epithelial cells by down-regulating the miR-145-5p/ NF-KB axis. Thus, this study provides a promising new strategy for the treatment of wet age-related macular degeneration. Fu *et al.* reported that HBEGF secreted by M2 macrophages could induce radioresistance to human papillomavirus negative head and neck squamous cell carcinoma.[43] Dong *et al.* reported that HBEGF promoted

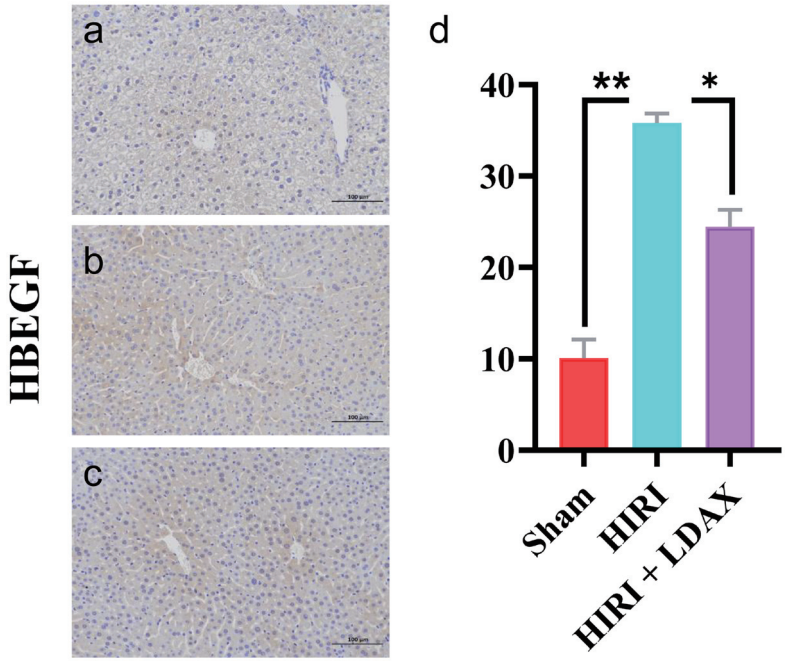

Fig. 5. HBEGF was verified by immunohistochemical. (a) Sham; (b) HIRI; (c) HIRI + LDAX. The scale is 100μm and the magnification is 200 times. e is the expression of HBEGF among groups analyzed by one-way ANOVA and Tukey's post-hoc statistical method, expressed as mean +SD ($\bar{x} \pm s$). Compared with HIRI group, HBEGF expression decreased in (HIRI + LDAX) group (*$P < 0.05$). Compared with Sham group, HBEGF expression in HIRI group was significantly increased (**$P < 0.01$). HBEGF, heparin-binding epidermal growth factor; HIRI, hepatic ischemia-reperfusion injury.

a

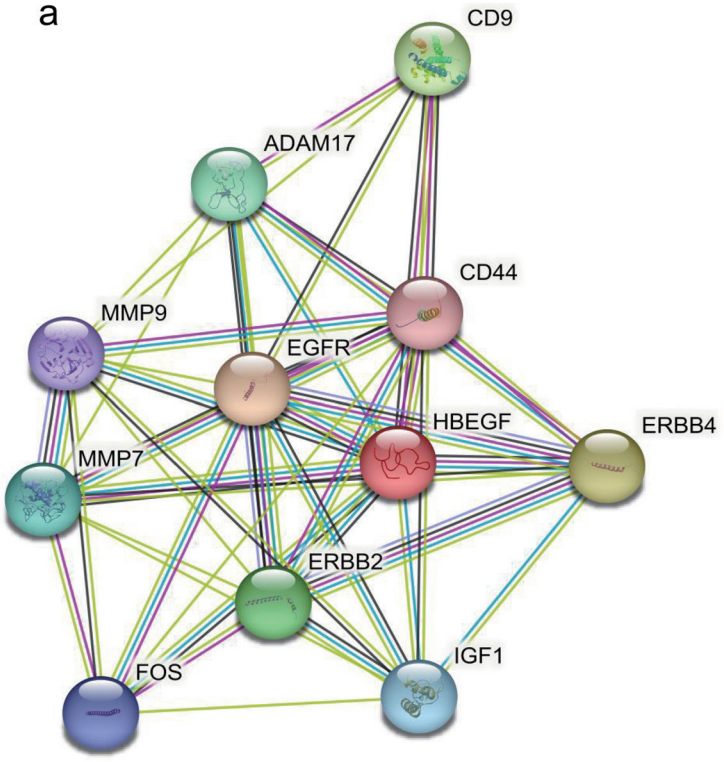

b

#node1	node2	Combined score
CD44	ERBB2	0.999
EGFR	HBEGF	0.999
ERBB4	HBEGF	0.999
EGFR	ERBB2	0.998
CD44	EGFR	0.997
CD44	MMP9	0.996
CD9	HBEGF	0.987
ERBB2	ERBB4	0.987
EGFR	FOS	0.977
EGFR	ERBB4	0.976
CD44	MMP7	0.975
ERBB2	HBEGF	0.97
ADAM17	HBEGF	0.968
HBEGF	IGF1	0.961
HBEGF	MMP7	0.961
ADAM17	ERBB4	0.959
FOS	HBEGF	0.958
HBEGF	MMP9	0.95
ADAM17	EGFR	0.949
ADAM17	ERBB2	0.948
CD44	HBEGF	0.948

Fig. 6. HBEGF protein interaction correlation diagram. (a) HBEGF target protein interaction map obtained from STRING database; (b) The combined score between HBEGF and its associated target protein. HBEGF, heparin-binding epidermal growth factor.

the proliferation and invasion of hepatocellular carcinoma (HCC) through the EGF receptor/phosphoinositol 3-kinase /Akt signaling pathway.[44] Meanwhile, the transmembrane protease Serine 4 can regulate HBEGF to promote HCC proliferation, invasion and angiogenesis, and HBEGF inhibitor 197 combined with sorafenib can be used for individualized treatment of HCC. It is suggested that HBEGF could be a potential therapeutic target for HCC. Choi *et al.* reported that HBEGF stimulated dermal papilla cells by increasing the dynamic and paracrine effects of adipogenic stem cells that released throboietin growth factor,[45] which promoted hair growth. The production of Reactive oxygen species and Hck Phosphorylation are the key factors for HBEGF-induced adipogenic stem cell stimulation. The production of Reactive oxygen species and Hck Phosphorylation are the key factors for HBEGF-induced adipogenic stem cell stimulation. Therefore, the combination of HBEGF and adipose-derived stem cells may provide a new solution for the treatment of hair loss. Farahnak *et al.* reported that the intrinsic HBEGF expressed by CD4 T cells had immunomodulatory functions in T(H)2 inflammation and airway dysfunction,[46] and the mechanism was mainly to regulate the expression of IL-5 by binding to and inhibiting the inhibitory function of Bcl-6. Yu *et al.* reported that HBEGF prevented the apoptosis of stromal cells by enhancing the activities of antioxidant enzymes SOD, CAT and GPX, inhibiting the activity of Caspase-3 and the expression of Bax, and restoring the mRNA level of Bcl-2 to improve the oxidative stress-mediated decidua injury.[47] Kushwaha *et al.* reported that rosiglitazone may protect the brain through peroxisome proliferator-activated receptor gamma-dependent HBEGF/EGFR signaling pathway and increased glial fibrillary acid protein.[48] In conclusion, the expression of HBEGF in various disease progression is not the same, and the expression of HBEGF in tumor and liver injury and other diseases is up-regulated, which is consistent with our experimental results. That is, with the intervention, the related symptoms are relieved as HBEGF is lowered. However, as reported above, upregulation of HBEGF is beneficial for immune regulatory functions in T(H)2 inflammation and airway dysfunction. It has also been reported that the combination of upregulation of HBEGF and adipose-derived stem cells provides a new technique for the treatment of hair loss. To sum up, the expression trend of HBEGF in different diseases is different, and the certainty of these data still needs to be verified by basic and clinical researchers with a large number of experimental data. In the future, the target gene HBEGF will make greater contribution to the diagnosis and treatment of many diseases.

In this study, two doses of DAX (5 g/kg and 2.5 g/kg) were selected to determine the pharmacodynamic effects of DAX on HIRI by observing the expressions of AST and ALT. The results showed that, compared with the model group, the expressions of AST and ALT were significantly decreased in the two DAX dose groups ($^{**}P < 0.01$), but there was no difference between the two DAX dose groups ($P > 0.05$), that is, there was no dose dependence. Therefore, the dosing of DAX will be our next in-depth discussion.

Conclusion

DAX protects HIRI in mice by down-regulating HBEGF expression. To provide theory for clinical study of new strategies for prevention and treatment of HIRI.

Acknowledgments

Authors thank the Central Laboratory of Tianjin First Central Hospital of China for providing the experimental site.

Funding

This work was financially supported by the Health Commission of Tianjin, China (ZC20215).

Conflict of interest

Hongsheng Liu is the editorial board member of *Future Integrative Medicine*. Other authors declare that they do not have competing interests regarding this publication.

Author contributions

HL conceived the overall idea of this project and completed the simulation experiment of receptor-ligand molecular docking. CG and ZL completed the data mining experiment of network pharmacology and RNA-seq. CG wrote the manuscript and HL corrected it. In short, all the authors agreed on the final version of the manuscript.

Ethics statement

The animal study was reviewed and approved by Animal Ethics Committee of Nankai University (license number: SCXK (Jing) 2014-0004).

Data sharing statement

The data used in support of the findings of this study are available from the corresponding author upon request.

References

[1] Ding MJ, Fang HR, Zhang JK, Shi JH, Yu X, Wen PH, *et al*. E3 ubiquitin ligase ring finger protein 5 protects against hepatic ischemia reperfusion injury by mediating phosphoglycerate mutase family member 5 ubiquitination. Hepatology 2022;76(1):94–111. doi:10.1002/hep.32226, PMID:34735734.

[2] Huang J, Xian S, Liu Y, Chen X, Pu K, Wang H. A Renally Clearable Activatable Polymeric Nanoprobe for Early Detection of Hepatic Ischemia-Reperfusion Injury. Adv Mater 2022;34(24):e2201357. doi:10.1002/adma.202201357, PMID:35436014.

[3] Zhou J, Hu M, He M, Wang X, Sun D, Huang Y, *et al*. TNFAIP3 Interacting Protein 3 Is an Activator of Hippo-YAP Signaling Protecting Against Hepatic Ischemia/Reperfusion Injury. Hepatology 2021;74(4):2133–2153. doi:10.1002/hep.32015, PMID:34133792.

[4] Zhu L, Zhou H, Xu F, Yang H, Li P, Sheng Y, *et al*. Hepatic Ischemia-Reperfusion Impairs Blood-Brain Barrier Partly Due to Release of Arginase From Injured Liver. Front Pharmacol 2021;12:724471. doi:10.3389/fphar.2021.724471, PMID:34721021.

[5] Kan C, Ungelenk L, Lupp A, Dirsch O, Dahmen U. Ischemia-Reperfusion Injury in Aged Livers-The Energy Metabolism, Inflammatory Response, and Autophagy. Transplantation 2018;102(3):368–377. doi:10.1097/TP.0000000000001999, PMID:29135887.

[6] Piao C, Zhang Q, Xu J, Wang Y, Liu T, Ma H, *et al*. Optimal intervention time of ADSCs for hepatic ischemia-reperfusion combined with partial resection injury in rats. Life Sci 2021;285:119986. doi:10.1016/j.lfs.2021.119986, PMID:34592233.

[7] Guan Y, Yao W, Yi K, Zheng C, Lv S, Tao Y, *et al*. Nanotheranostics for the Management of Hepatic Ischemia-Reperfusion Injury. Small 2021;17(23):e2007727. doi:10.1002/smll.202007727, PMID:33852769.

[8] Ma T, Zhang H, Li T, Bai J, Wu Z, Cai T, *et al*. Protective effect of pi-

nocembrin from Penthorum chinense Pursh on hepatic ischemia reperfusion injury via regulating HMGB1/TLR4 signal pathway. Phytother Res 2023;37(1):181–194. doi:10.1002/ptr.7605, PMID:36097366.
[9] Zhu SF, Yuan W, Du YL, Wang BL. Research progress of lncRNA and miRNA in hepatic ischemia-reperfusion injury. Hepatobiliary Pancreat Dis Int 2023;22(1):45–53. doi:10.1016/j.hbpd.2022.07.008, PMID:35934611.
[10] Gao W, Feng Z, Zhang S, Wu B, Geng X, Fan G, *et al*. Anti-Inflammatory and Antioxidant Effect of Eucommia ulmoides Polysaccharide in Hepatic Ischemia-Reperfusion Injury by Regulating ROS and the TLR-4-NF-κB Pathway. Biomed Res Int 2020;2020:1860637. doi:10.1155/2020/1860637, PMID:32566664.
[11] He D, Guo Z, Pu JL, Zheng DF, Wei XF, Liu R, *et al*. Resveratrol preconditioning protects hepatocytes against hepatic ischemia reperfusion injury via Toll-like receptor 4/nuclear factor-κB signaling pathway in vitro and in vivo. Int Immunopharmacol 2016;35:201–209. doi:10.1016/j.intimp.2016.03.032, PMID:27064547.
[12] Zhang H, Gao W Z. Effects of salidroside on liver injury and Bcl?2 and Bax in hepatic ischemia-reperfusion rats. Mod Med Hyg 2018;5(34):690–692. doi:10.3969/j.issn.1009-5519.2018.05.014.
[13] Hopkins AL. Network pharmacology. Nat Biotechnol 2007;25(10):1110–1111. doi:10.1038/nbt1007-1110, PMID:17921993.
[14] Pan HT, Xi ZQ, Wei XQ, Wang K. A network pharmacology approach to predict potential targets and mechanisms of "Ramulus Cinnamomi (cassiae)-Paeonia lactiflora" herb pair in the treatment of chronic pain with comorbid anxiety and depression. Ann Med 2022;54(1):413–425. doi:10.1080/07853890.2022.2031268, PMID:35098831.
[15] Jun L, Yong MH, Hui W. Advances in network pharmacology. West China J Pharm Sci 2014;29(6):723–725.
[16] Gao X, Liu Y, An Z, Ni J. Active Components and Pharmacological Effects of Cornus officinalis: Literature Review. Front Pharmacol 2021;12:633447. doi:10.3389/fphar.2021.633447, PMID:33912050.
[17] Xin JI, Qi SC, Ling PG. Advances in pharmacology of Cornus officinalis. J Liaoning University of Chinese Medicine 2022;24(4):63–66.
[18] Xu JJ, Li RJ, Zhang ZH, Yang C, Liu SX, Li YL, *et al*. Loganin Inhibits Angiotensin II-Induced Cardiac Hypertrophy Through the JAK2/STAT3 and NF-κB Signaling Pathways. Front Pharmacol 2021;12:678886. doi:10.3389/fphar.2021.678886, PMID:34194329.
[19] Hu JM, Chen Q, Xiao LW, Dong PJ, Wu CL, Yuan HF. Advances in pharmacological action and mechanism of loganin. Chinese Journal of Basic Medicine of TCL 2020;26(08):1206–1209. doi:10.3969/j.issn.1006-3250.2020.08.052.
[20] Zhang JZ, Li LM, Huang L, Ning N, Liu Y. Effect of Banxia Xiexin Decoction and its dissolving recipe on gastrin and somatostatin in spleen-deficient rats. Pharmacol Clin Chin Mater Med 2013;29(01):15–17. doi:CNKI:SUN:ZYYL.0.2013-01-005.
[21] Zhao T, Lv G, Liu B, Wu J, Di L, Yao Y, *et al*. Inventor; Nanjing University of Chinese Medicine, assignee. Use of dogwood loganin in preparing medicine for treating diabetes mellitus. P. R. China Patent CN103110651-A. 2013 November.
[22] Wan H, Li C, Yang Y, Chen D. Loganin attenuates interleukin-1β-induced chondrocyte inflammation, cartilage degeneration, and rat synovial inflammation by regulating TLR4/MyD88/NF-κB. J Int Med Res 2022;50(8):3000605221104764. doi:10.1177/03000605221104764, PMID:36000146.
[23] Choi YH. Activation of Nrf2/HO-1 antioxidant signaling correlates with the preventive effect of loganin on oxidative injury in ARPE-19 human retinal pigment epithelial cells. Genes Genomics 2023;45(3):271–284. doi:10.1007/s13258-022-01302-4, PMID:36018494.
[24] Choi N, Yang G, Jang JH, Kang HC, Cho YY, Lee HS, *et al*. Loganin Alleviates Gout Inflammation by Suppressing NLRP3 Inflammasome Activation and Mitochondrial Damage. Molecules 2021;26(4):1071. doi:10.3390/molecules26041071, PMID:33670601.
[25] Chen C, Ai Q, Shi A, Wang N, Wang L, Wei Y. Oleanolic acid and ursolic acid: therapeutic potential in neurodegenerative diseases, neuropsychiatric diseases and other brain disorders. Nutr Neurosci 2023;26(5):414–428. doi:10.1080/1028415X.2022.2051957, PMID:35311613.
[26] Shi Y, Leng Y, Liu D, Liu X, Ren Y, Zhang J, *et al*. Research Advances in Protective Effects of Ursolic Acid and Oleanolic Acid Against Gastrointestinal Diseases. Am J Chin Med 2021;49(2):413–435. doi:10.1142/S0192415X21500191, PMID:33622215.
[27] Fan JP, Lai XH, Zhang XH, Yang L, Yuan TT, Chen HP, *et al*. Synthesis and evaluation of the cancer cell growth inhibitory activity of the ionic derivatives of oleanolic acid andursolic acid with improved solubility. J Mol Liq 2021;332:115837. doi:10.1016/j.molliq.2021.115837.
[28] Castrejón-Jiménez NS, Leyva-Paredes K, Baltierra-Uribe SL, Castillo-Cruz J, Campillo-Navarro M, Hernández-Pérez AD, *et al*. Ursolic and Oleanolic Acids Induce Mitophagy in A549 Human Lung Cancer Cells. Molecules 2019;24(19):3444. doi:10.3390/molecules24193444, PMID:31547522.
[29] Liu CM, Huang JY, Sheng LX, Wen XA, Cheng KG. Synthesis and antitumor activity of fluorouracil - oleanolic acid/ursolic acid/glycyrrhetinic acid conjugates. Medchemcomm 2019;10(8):1370–1378. doi:10.1039/c9md00246d, PMID:31673307.
[30] Piet M, Paduch R. Ursolic and oleanolic acids as potential anticancer agents acting in the gastrointestinal tract. Mini-Rev Org Chem 2019;16(1):78–91. doi:10.2174/1570193x15666180612090816.
[31] Czerwińska ME, Bobińska A, Cichocka K, Buchholz T, Woliński K, Melzig MF. Cornus mas and Cornus officinalis-A Comparison of Antioxidant and Immunomodulatory Activities of Standardized Fruit Extracts in Human Neutrophils and Caco-2 Models. Plants (Basel) 2021;10(11):2347. doi:10.3390/plants10112347, PMID:34834710.
[32] Yang J, Cao B, Xue Y, Liang H, Wu Y, Zhao N, *et al*. The medicinal active ingredients and their associated key enzyme genes are differentially regulated at different growth stages in Cornus officinalis and Cornus controversa. Ind Crop Prod 2019;142:111858. doi:10.1016/j.indcrop.2019.111858.
[33] Guo YX, Zhang Y, Gao YH, Deng SY, Wang LM, Li CQ, *et al*. Role of Plant-Derived Natural Compounds in Experimental Autoimmune Encephalomyelitis: A Review of the Treatment Potential and Development Strategy. Front Pharmacol 2021;12:639651. doi:10.3389/fphar.2021.639651, PMID:34262447.
[34] Hou W, Wei B, Liu HS. The Protective Effect of Panax notoginseng Mixture on Hepatic Ischemia/Reperfusion Injury in Mice via Regulating NR3C2, SRC, and GAPDH. Front Pharmacol 2021;12:756259. doi:10.3389/fphar.2021.756259, PMID:34858181.
[35] Zhang JJ, Cao CX, Wan LL, Zhang W, Liu ZJ, Wang JL, *et al*. Forkhead Box q1 promotes invasion and metastasis in colorectal cancer by activating the epidermal growth factor receptor pathway. World J Gastroenterol 2022;28(17):1781–1797. doi:10.3748/wjg.v28.i17.1781, PMID:35633908.
[36] Sakamoto T, Pak K, Chavez E, Ryan AF, Kurabi A. HB-EGF Plays a Pivotal Role in Mucosal Hyperplasia During Otitis Media Induced by a Viral Analog. Front Cell Infect Microbiol 2022;12:823714. doi:10.3389/fcimb.2022.823714, PMID:35281434.
[37] Wang J, Zhang Y, Zhang G, Xiang L, Pang H, Xiong K, *et al*. Radiotherapy-induced enrichment of EGF-modified doxorubicin nanoparticles enhances the therapeutic outcome of lung cancer. Drug Deliv 2022;29(1):588–599. doi:10.1080/10717544.2022.2036871, PMID:35156493.
[38] Zhang B, Liu Q, Wen W, Gao H, Wei W, Tang A, *et al*. The chromatin remodeler CHD6 promotes colorectal cancer development by regulating TMEM65-mediated mitochondrial dynamics via EGF and Wnt signaling. Cell Discov 2022;8(1):130. doi:10.1038/s41421-022-00478-z, PMID:36473865.
[39] Van Hiep N, Sun WL, Feng PH, Lin CW, Chen KY, Luo CS, *et al*. Heparin binding epidermal growth factor-like growth factor is a prognostic marker correlated with levels of macrophages infiltrated in lung adenocarcinoma. Front Oncol 2022;12:963896. doi:10.3389/fonc.2022.963896, PMID:36439487.
[40] Li Y, Su G, Zhong Y, Xiong Z, Huang T, Quan J, *et al*. HB-EGF-induced IL-8 secretion from airway epithelium leads to lung fibroblast proliferation and migration. BMC Pulm Med 2021;21(1):347. doi:10.1186/s12890-021-01726-w, PMID:34742261.
[41] Salama Y, Jaradat N, Hattori K, Heissig B. Aloysia Citrodora Essential Oil Inhibits Melanoma Cell Growth and Migration by Targeting HB-EGF-EGFR Signaling. Int J Mol Sci 2021;22(15):8151. doi:10.3390/ijms22158151, PMID:34360915.
[42] Gu J, Qiu Z, Li L, Qin B, Zhou Y, Liu Y, *et al*. Geniposide alleviates choroidal neovascularization by downregulating HB-EGF release from RPE cells by downregulating the miR-145-5p/NF-κB axis. Exp Eye Res 2021;208:108624. doi:10.1016/j.exer.2021.108624,

PMID:34022175.
[43] Fu E, Liu T, Yu S, Chen X, Song L, Lou H, *et al*. M2 macrophages reduce the radiosensitivity of head and neck cancer by releasing HB-EGF. Oncol Rep 2020;44(2):698–710. doi:10.3892/or.2020.7628, PMID:32627036.
[44] Dong ZR, Sun D, Yang YF, Zhou W, Wu R, Wang XW, *et al*. TMPRSS4 Drives Angiogenesis in Hepatocellular Carcinoma by Promoting HB-EGF Expression and Proteolytic Cleavage. Hepatology 2020;72(3):923–939. doi:10.1002/hep.31076, PMID:31867749.
[45] Choi N, Kim WS, Oh SH, Sung JH. HB-EGF Improves the Hair Regenerative Potential of Adipose-Derived Stem Cells via ROS Generation and Hck Phosphorylation. Int J Mol Sci 2019;21(1):122. doi:10.3390/ijms21010122, PMID:31878047.
[46] Farahnak S, Simon L, McGovern TK, Chen M, Khazaei N, Martin JG. HB-EGF Synthesized by CD4 T Cells Modulates Allergic Airway Eosinophilia by Regulating IL-5 Synthesis. J Immunol 2019;203(1):39–47. doi:10.4049/jimmunol.1801686, PMID:31127030.
[47] Yu HF, Duan CC, Yang ZQ, Wang YS, Yue ZP, Guo B. HB-EGF Ameliorates Oxidative Stress-Mediated Uterine Decidualization Damage. Oxid Med Cell Longev 2019;2019:6170936. doi:10.1155/2019/6170936, PMID:31885807.
[48] Kushwaha R, Mishra J, Gupta AP, Gupta K, Vishwakarma J, Chattopadhyay N, *et al*. Rosiglitazone up-regulates glial fibrillary acidic protein via HB-EGF secreted from astrocytes and neurons through PPARγ pathway and reduces apoptosis in high-fat diet-fed mice. J Neurochem 2019;149(5):679–698. doi:10.1111/jnc.14610, PMID:30311190.